EUROPEAN ORGANIZATION FOR NUCLEAR RESEARCH

CERN–PPE/94-99

29 June 1994

J/ψ Production in the Hadronic Decays of the Z

DELPHI Collaboration

Abstract

J/ψ mesons have been reconstructed from their decay to $\mu^+\mu^-$ and e^+e^-, using the data collected by the DELPHI experiment during 1991 and 1992 at the LEP collider. From about 1 million hadronic Z decays 153 ± 17 J/ψ were found, 5.4 ± 2.3 ψ' were obtained in the channel $J/\psi(\rightarrow \mu^+\mu^-)\pi^+\pi^-$ and 6.4 ± 2.7 χ_c in the channel $J/\psi(\rightarrow \mu^+\mu^-)\gamma$. As the dominant source of J/ψ mesons is from b quarks, the following branching ratios:

$$Br(b \rightarrow J/\psi\ X) = (1.12 \pm 0.12\ (\text{stat.}) \pm 0.10\ (\text{syst.}))\%$$

$$Br(b \rightarrow \psi'\ X) = (0.48 \pm 0.22\ (\text{stat.}) \pm 0.10\ (\text{syst.}))\%$$

$$Br(b \rightarrow \chi_{c1}\ X) = (1.4 \pm 0.6\ (\text{stat.})^{+0.4}_{-0.2}\ (\text{syst.}))\%$$

were measured. From the proper time distribution of the J/ψ sample, the average lifetime of b-hadrons decaying into J/ψ was found to be:

$$\tau_B = 1.50^{+0.24}_{-0.21}\ (\text{stat.}) \pm 0.03\ (\text{syst.})\ \text{ps}.$$

A search for completely reconstructed B meson decays to final states including a J/ψ gave a signal of 15 ± 5 events.

(Submitted to Physics Letters B)

P.Abreu[20], W.Adam[7], T.Adye[37], E.Agasi[30], I.Ajinenko[42], R.Aleksan[39], G.D.Alekseev[14], P.P.Allport[21], S.Almehed[23], F.M.L.Almeida[47], S.J.Alvsvaag[4], U.Amaldi[7], A.Andreazza[27], P.Antilogus[24], W-D.Apel[15], R.J.Apsimon[37], Y.Arnoud[39], B.Åsman[44], J-E.Augustin[18], A.Augustinus[30], P.Baillon[7], P.Bambade[18], F.Barao[20], R.Barate[12], G.Barbiellini[46], D.Y.Bardin[14], G.J.Barker[34], A.Baroncelli[40], O.Barring[7], J.A.Barrio[25], W.Bartl[50], M.J.Bates[37], M.Battaglia[13], M.Baubillier[22], J.Baudot[39], K-H.Becks[52], M.Begalli[36], P.Beilliere[6], P.Beltran[9], A.C.Benvenuti[5], M.Berggren[41], D.Bertrand[2], F.Bianchi[45], M.Bigi[45], M.S.Bilenky[14], P.Billoir[22], J.Bjarne[23], D.Bloch[8], J.Blocki[51], S.Blyth[34], V.Bocci[38], P.N.Bogolubov[14], T.Bolognese[39], M.Bonesini[27], W.Bonivento[27], P.S.L.Booth[21], G.Borisov[42], C.Bosio[40], B.Bostjancic[43], S.Bosworth[34], O.Botner[48], B.Bouquet[18], C.Bourdarios[18], T.J.V.Bowcock[21], M.Bozzo[11], S.Braibant[2], P.Branchini[40], K.D.Brand[35], R.A.Brenner[13], H.Briand[22], C.Bricman[2], L.Brillault[22], R.C.A.Brown[7], P.Bruckman[16], J-M.Brunet[6], L.Bugge[32], T.Buran[32], A.Buys[7], J.A.M.A.Buytaert[7], M.Caccia[27], M.Calvi[27], A.J.Camacho Rozas[41], R.Campion[21], T.Camporesi[7], V.Canale[38], K.Cankocak[44], F.Cao[2], F.Carena[7], P.Carrilho[47], L.Carroll[21], R.Cases[49], C.Caso[11], M.V.Castillo Gimenez[49], A.Cattai[7], F.R.Cavallo[5], L.Cerrito[38], V.Chabaud[7], A.Chan[1], M.Chapkin[42], Ph.Charpentier[7], L.Chaussard[24], J.Chauveau[22], P.Checchia[35], G.A.Chelkov[14], P.Chliapnikov[42], V.Chorowicz[22], J.T.M.Chrin[49], V.Cindro[43], P.Collins[34], J.L.Contreras[18], R.Contri[11], E.Cortina[49], G.Cosme[18], F.Couchot[18], H.B.Crawley[1], D.Crennell[37], G.Crosetti[11], J.Cuevas Maestro[33], S.Czellar[13], E.Dahl-Jensen[28], J.Dahm[52], B.Dalmagne[18], M.Dam[32], G.Damgaard[28], E.Daubie[2], A.Daum[15], P.D.Dauncey[37], M.Davenport[7], J.Davies[21], W.Da Silva[22], C.Defoix[6], P.Delpierre[26], N.Demaria[34], A.De Angelis[7], H.De Boeck[2], W.De Boer[15], S.De Brabandere[2], C.De Clercq[2], M.D.M.De Fez Laso[49], C.De La Vaissiere[22], B.De Lotto[46], A.De Min[27], L.De Paula[47], C.De Saint-Jean[39], H.Dijkstra[7], L.Di Ciaccio[38], F.Djama[8], J.Dolbeau[6], M.Donszelmann[7], K.Doroba[51], M.Dracos[8], J.Drees[52], M.Dris[31], Y.Dufour[7], F.Dupont[12], D.Edsall[1], R.Ehret[15], T.Ekelof[48], G.Ekspong[44], M.Elsing[52], J-P.Engel[8], N.Ershaidat[22], M.Espirito Santo[20], D.Fassouliotis[31], M.Feindt[7], A.Ferrer[49], T.A.Filippas[31], A.Firestone[1], H.Foeth[7], E.Fokitis[31], F.Fontanelli[11], F.Formenti[7], J-L.Fousset[26], B.Franek[37], P.Frenkiel[6], D.C.Fries[15], A.G.Frodesen[4], R.Fruhwirth[50], F.Fulda-Quenzer[18], H.Furstenau[7], J.Fuster[7], D.Gamba[45], M.Gandelman[17], C.Garcia[49], J.Garcia[41], C.Gaspar[7], U.Gasparini[35], Ph.Gavillet[7], E.N.Gazis[31], D.Gele[8], J-P.Gerber[8], P.Giacomelli[7], D.Gillespie[7], R.Gokieli[51], B.Golob[43], V.M.Golovatyuk[14], J.J.Gomez Y Cadenas[7], G.Gopal[37], L.Gorn[1], M.Gorski[51], V.Gracco[11], F.Grard[2], E.Graziani[40], G.Grosdidier[18], P.Gunnarsson[44], J.Guy[37], U.Haedinger[15], F.Hahn[52], M.Hahn[44], S.Hahn[52], S.Haider[30], Z.Hajduk[16], A.Hakansson[23], A.Hallgren[48], K.Hamacher[52], W.Hao[30], F.J.Harris[34], V.Hedberg[23], R.Henriques[20], J.J.Hernandez[49], J.A.Hernando[49], P.Herquet[2], H.Herr[7], T.L.Hessing[21], E.Higon[49], H.J.Hilke[7], T.S.Hill[1], S-O.Holmgren[44], P.J.Holt[34], D.Holthuizen[30], P.F.Honore[6], M.Houlden[21], K.Huet[2], K.Hultqvist[44], P.Ioannou[3], P-S.Iversen[4], J.N.Jackson[21], R.Jacobsson[44], P.Jalocha[16], G.Jarlskog[23], P.Jarry[39], B.Jean-Marie[18], E.K.Johansson[44], M.Jonker[7], L.Jonsson[23], P.Juillot[8], M.Kaiser[15], G.Kalmus[37], F.Kapusta[22], M.Karlsson[44], E.Karvelas[9], A.Katargin[42], S.Katsanevas[3], E.C.Katsoufis[31], R.Keranen[7], B.A.Khomenko[14], N.N.Khovanski[14], B.King[21], N.J.Kjaer[28], H.Klein[7], A.Klovning[4], P.Kluit[30], A.Koch-Mehrin[52], J.H.Koehne[15], B.Koene[30], P.Kokkinias[9], M.Koratzinos[32], A.V.Korytov[14], V.Kostioukhine[42], C.Kourkoumelis[3], O.Kouznetsov[14], P.-H.Kramer[52], M.Krammer[50], C.Kreuter[15], J.Krolikowski[51], I.Kronkvist[23], W.Krupinski[16], W.Kucewicz[16], K.Kulka[48], K.Kurvinen[13], C.Lacasta[49], I.Laktineh[24], C.Lambropoulos[9], J.W.Lamsa[1], L.Lanceri[46], P.Langefeld[52], V.Lapin[42], I.Last[21], J-P.Laugier[39], R.Lauhakangas[13], G.Leder[50], F.Ledroit[12], R.Leitner[29], Y.Lemoigne[39], J.Lemonne[2], G.Lenzen[52], V.Lepeltier[18], T.Lesiak[35], J.M.Levy[8], E.Lieb[52], D.Liko[50], R.Lindner[52], A.Lipniacka[18], I.Lippi[35], B.Loerstad[23], M.Lokajicek[10], J.G.Loken[34], A.Lopez-Fernandez[7], M.A.Lopez Aguera[41], M.Los[30], D.Loukas[9], J.J.Lozano[49], P.Lutz[39], L.Lyons[34], G.Maehlum[15], J.Maillard[6], A.Maio[20], A.Maltezos[9], F.Mandl[50], J.Marco[41], B.Marechal[47], M.Margoni[35], J-C.Marin[7], C.Mariotti[40], A.Markou[9], T.Maron[52], S.Marti[49], C.Martinez-Rivero[41], F.Martinez-Vidal[49], F.Matorras[41], C.Matteuzzi[27], G.Matthiae[38], M.Mazzucato[35], M.Mc Cubbin[21], R.Mc Kay[1], R.Mc Nulty[21], J.Medbo[48], C.Meroni[27], W.T.Meyer[1], M.Michelotto[35], E.Migliore[45], I.Mikulec[50], L.Mirabito[24], W.A.Mitaroff[50], G.V.Mitselmakher[14], U.Mjoernmark[23], T.Moa[44], R.Moeller[28], K.Moenig[7], M.R.Monge[11], P.Morettini[11], H.Mueller[15], W.J.Murray[37], B.Muryn[16], G.Myatt[34], F.Naraghi[12], F.L.Navarria[5], P.Negri[27], S.Nemecek[10], W.Neumann[52], N.Neumeister[50], R.Nicolaidou[3], B.S.Nielsen[28], V.Nikolaenko[24], P.Niss[44], A.Nomerotski[35], A.Normand[34], V.Obraztsov[42], A.G.Olshevski[14], R.Orava[13], K.Osterberg[13], A.Ouraou[39], P.Paganini[18], M.Paganoni[27], R.Pain[22], H.Palka[16], Th.D.Papadopoulou[31], L.Pape[7], F.Parodi[11], A.Passeri[40], M.Pegoraro[35], J.Pennanen[13], L.Peralta[20], H.Pernegger[50], M.Pernicka[50], A.Perrotta[5], C.Petridou[46], A.Petrolini[11], H.T.Phillips[37], G.Piana[11], F.Pierre[39], M.Pimenta[20], S.Plaszczynski[18], O.Podobrin[15], M.E.Pol[17], G.Polok[16], P.Poropat[46], V.Pozdniakov[14], M.Prest[46], P.Privitera[38], A.Pullia[27], D.Radojicic[34], S.Ragazzi[27], H.Rahmani[31], J.Rames[10], P.N.Ratoff[19], A.L.Read[32], M.Reale[52], P.Rebecchi[18], N.G.Redaelli[27], M.Regler[50], D.Reid[7], P.B.Renton[34], L.K.Resvanis[3], F.Richard[18], J.Richardson[21], J.Ridky[10], G.Rinaudo[45], I.Ripp[39], A.Romero[45], I.Roncagliolo[11], P.Ronchese[35], L.Roos[12], E.I.Rosenberg[1], E.Rosso[7], P.Roudeau[18], T.Rovelli[5], W.Ruckstuhl[30], V.Ruhlmann-Kleider[39], A.Ruiz[41], H.Saarikko[13], Y.Sacquin[39], G.Sajot[12], J.Salt[49], J.Sanchez[25], M.Sannino[11], S.Schael[7], H.Schneider[15], M.A.E.Schyns[52], G.Sciolla[45], F.Scuri[46], A.M.Segar[34], A.Seitz[15], R.Sekulin[37], M.Sessa[46], R.Seufert[15], R.C.Shellard[36], I.Siccama[30], P.Siegrist[39], S.Simonetti[39], F.Simonetto[35], A.N.Sisakian[14], T.B.Skaali[32], G.Smadja[24], N.Smirnov[42], O.Smirnova[14], G.R.Smith[37], R.Sosnowski[51], D.Souza-Santos[36], T.Spassov[20], E.Spiriti[40], S.Squarcia[11], H.Staeck[52], C.Stanescu[40], S.Stapnes[32], I.Stavitski[35], G.Stavropoulos[9], K.Stepaniak[51], F.Stichelbaut[7], A.Stocchi[18], J.Strauss[50], J.Straver[7], R.Strub[8], B.Stugu[4], M.Szczekowski[51], M.Szeptycka[51],

T.Tabarelli[27], O.Tchikilev[42], G.E.Theodosiou[9], Z.Thome[47], A.Tilquin[26], J.Timmermans[30], V.G.Timofeev[14], L.G.Tkatchev[14], T.Todorov[8], D.Z.Toet[30], A.Tomaradze[2], B.Tome[20], E.Torassa[45], L.Tortora[40], G.Transtromer[23], D.Treille[7], W.Trischuk[7], G.Tristram[6], C.Troncon[27], A.Tsirou[7], E.N.Tsyganov[14], M-L.Turluer[39], T.Tuuva[13], I.A.Tyapkin[22], M.Tyndel[37], S.Tzamarias[21], B.Ueberschaer[52], S.Ueberschaer[52], O.Ullaland[7], V.Uvarov[42], G.Valenti[5], E.Vallazza[7], J.A.Valls Ferrer[49], C.Vander Velde[2], G.W.Van Apeldoorn[30], P.Van Dam[30], M.Van Der Heijden[30], W.K.Van Doninck[2], J.Van Eldik[30], P.Vaz[7], G.Vegni[27], L.Ventura[35], W.Venus[37], F.Verbeure[2], M.Verlato[35], L.S.Vertogradov[14], D.Vilanova[39], P.Vincent[24], L.Vitale[46], E.Vlasov[42], A.S.Vodopyanov[14], M.Vollmer[52], M.Voutilainen[13], V.Vrba[10], H.Wahlen[52], C.Walck[44], F.Waldner[46], A.Wehr[52], M.Weierstall[52], P.Weilhammer[7], A.M.Wetherell[7], J.H.Wickens[2], M.Wielers[15], G.R.Wilkinson[34], W.S.C.Williams[34], M.Winter[8], M.Witek[7], G.Wormser[18], K.Woschnagg[48], K.Yip[34], O.Yushchenko[42], F.Zach[24], A.Zaitsev[42], A.Zalewska[16], P.Zalewski[51], D.Zavrtanik[43], E.Zevgolatakos[9], N.I.Zimin[14], M.Zito[39], D.Zontar[43], R.Zuberi[34], G.Zumerle[35]

[1] Ames Laboratory and Department of Physics, Iowa State University, Ames IA 50011, USA
[2] Physics Department, Univ. Instelling Antwerpen, Universiteitsplein 1, B-2610 Wilrijk, Belgium
and IIHE, ULB-VUB, Pleinlaan 2, B-1050 Brussels, Belgium
and Faculté des Sciences, Univ. de l'Etat Mons, Av. Maistriau 19, B-7000 Mons, Belgium
[3] Physics Laboratory, University of Athens, Solonos Str. 104, GR-10680 Athens, Greece
[4] Department of Physics, University of Bergen, Allégaten 55, N-5007 Bergen, Norway
[5] Dipartimento di Fisica, Università di Bologna and INFN, Via Irnerio 46, I-40126 Bologna, Italy
[6] Collège de France, Lab. de Physique Corpusculaire, IN2P3-CNRS, F-75231 Paris Cedex 05, France
[7] CERN, CH-1211 Geneva 23, Switzerland
[8] Centre de Recherche Nucléaire, IN2P3 - CNRS/ULP - BP20, F-67037 Strasbourg Cedex, France
[9] Institute of Nuclear Physics, N.C.S.R. Demokritos, P.O. Box 60228, GR-15310 Athens, Greece
[10] FZU, Inst. of Physics of the C.A.S. High Energy Physics Division, Na Slovance 2, 180 40, Praha 8, Czech Republic
[11] Dipartimento di Fisica, Università di Genova and INFN, Via Dodecaneso 33, I-16146 Genova, Italy
[12] Institut des Sciences Nucléaires, IN2P3-CNRS, Université de Grenoble 1, F-38026 Grenoble Cedex, France
[13] Research Institute for High Energy Physics, SEFT, P.O. Box 9, FIN-00014 Helsinki, Finland
[14] Joint Institute for Nuclear Research, Dubna, Head Post Office, P.O. Box 79, 101 000 Moscow, Russian Federation
[15] Institut für Experimentelle Kernphysik, Universität Karlsruhe, Postfach 6980, D-76128 Karlsruhe, Germany
[16] High Energy Physics Laboratory, Institute of Nuclear Physics, Ul. Kawiory 26a, PL-30055 Krakow 30, Poland
[17] Centro Brasileiro de Pesquisas Físicas, rua Xavier Sigaud 150, BR-22290 Rio de Janeiro, Brazil
[18] Université de Paris-Sud, Lab. de l'Accélérateur Linéaire, IN2P3-CNRS, Bat 200, F-91405 Orsay Cedex, France
[19] School of Physics and Materials, University of Lancaster, Lancaster LA1 4YB, UK
[20] LIP, IST, FCUL - Av. Elias Garcia, 14-1°, P-1000 Lisboa Codex, Portugal
[21] Department of Physics, University of Liverpool, P.O. Box 147, Liverpool L69 3BX, UK
[22] LPNHE, IN2P3-CNRS, Universités Paris VI et VII, Tour 33 (RdC), 4 place Jussieu, F-75252 Paris Cedex 05, France
[23] Department of Physics, University of Lund, Sölvegatan 14, S-22363 Lund, Sweden
[24] Université Claude Bernard de Lyon, IPNL, IN2P3-CNRS, F-69622 Villeurbanne Cedex, France
[25] Universidad Complutense, Avda. Complutense s/n, E-28040 Madrid, Spain
[26] Univ. d'Aix - Marseille II - CPP, IN2P3-CNRS, F-13288 Marseille Cedex 09, France
[27] Dipartimento di Fisica, Università di Milano and INFN, Via Celoria 16, I-20133 Milan, Italy
[28] Niels Bohr Institute, Blegdamsvej 17, DK-2100 Copenhagen 0, Denmark
[29] NC, Nuclear Centre of MFF, Charles University, Areal MFF, V Holesovickach 2, 180 00, Praha 8, Czech Republic
[30] NIKHEF-H, Postbus 41882, NL-1009 DB Amsterdam, The Netherlands
[31] National Technical University, Physics Department, Zografou Campus, GR-15773 Athens, Greece
[32] Physics Department, University of Oslo, Blindern, N-1000 Oslo 3, Norway
[33] Dpto. Fisica, Univ. Oviedo, C/P. Pérez Casas, S/N-33006 Oviedo, Spain
[34] Department of Physics, University of Oxford, Keble Road, Oxford OX1 3RH, UK
[35] Dipartimento di Fisica, Università di Padova and INFN, Via Marzolo 8, I-35131 Padua, Italy
[36] Depto. de Fisica, Pontificia Univ. Católica, C.P. 38071 RJ-22453 Rio de Janeiro, Brazil
[37] Rutherford Appleton Laboratory, Chilton, Didcot OX11 OQX, UK
[38] Dipartimento di Fisica, Università di Roma II and INFN, Tor Vergata, I-00173 Rome, Italy
[39] Centre d'Etude de Saclay, DSM/DAPNIA, F-91191 Gif-sur-Yvette Cedex, France
[40] Istituto Superiore di Sanità, Ist. Naz. di Fisica Nucl. (INFN), Viale Regina Elena 299, I-00161 Rome, Italy
[41] C.E.A.F.M., C.S.I.C. - Univ. Cantabria, Avda. los Castros, S/N-39006 Santander, Spain, (CICYT-AEN93-0832)
[42] Inst. for High Energy Physics, Serpukov P.O. Box 35, Protvino, (Moscow Region), Russian Federation
[43] J. Stefan Institute and Department of Physics, University of Ljubljana, Jamova 39, SI-61000 Ljubljana, Slovenia
[44] Fysikum, Stockholm University, Box 6730, S-113 85 Stockholm, Sweden
[45] Dipartimento di Fisica Sperimentale, Università di Torino and INFN, Via P. Giuria 1, I-10125 Turin, Italy
[46] Dipartimento di Fisica, Università di Trieste and INFN, Via A. Valerio 2, I-34127 Trieste, Italy
and Istituto di Fisica, Università di Udine, I-33100 Udine, Italy
[47] Univ. Federal do Rio de Janeiro, C.P. 68528 Cidade Univ., Ilha do Fundão BR-21945-970 Rio de Janeiro, Brazil
[48] Department of Radiation Sciences, University of Uppsala, P.O. Box 535, S-751 21 Uppsala, Sweden
[49] IFIC, Valencia-CSIC, and D.F.A.M.N., U. de Valencia, Avda. Dr. Moliner 50, E-46100 Burjassot (Valencia), Spain
[50] Institut für Hochenergiephysik, Österr. Akad. d. Wissensch., Nikolsdorfergasse 18, A-1050 Vienna, Austria
[51] Inst. Nuclear Studies and University of Warsaw, Ul. Hoza 69, PL-00681 Warsaw, Poland
[52] Fachbereich Physik, University of Wuppertal, Postfach 100 127, D-42097 Wuppertal 1, Germany

1 Introduction

J/ψ mesons are expected to be produced at LEP energies predominantly through the reaction

$$Z \to b\overline{b},\ b \to J/\psi\ X. \tag{1}$$

Other production mechanisms may be gluon fragmentation :

$$Z \to q\bar{q}g^*, g^* \to J/\psi gg \tag{2}$$

or charm fragmentation :

$$Z \to J/\psi\ c\bar{c} \tag{3}$$

where one of the primary $c(\bar{c})$ quarks associates with a $\bar{c}(c)$ from a $c\bar{c}$ pair from the sea. In all these processes, J/ψ may be produced from cascade decays of higher charmonium states (ψ' or χ_c). Reactions (2) and (3) ("direct" J/ψ production) are theoretically expected to give small and approximately equal contributions, at the level of 1% of the rate from reaction (1), see [1], [2]. Therefore J/ψ events can be used to tag b decays and to measure the inclusive B lifetime, as well as the individual lifetimes of the various b-hadrons [3]-[5].

A brief description of the DELPHI apparatus and of the event selection is given in section 2. In section 3, lepton identification and selection of J/ψ, ψ' and χ_c are discussed. Results on inclusive branching ratios and lifetime are presented in sections 4 and 5.

2 Experimental procedure and event sample

This paper is based on the data collected in 1991 and 1992 by the DELPHI detector. The components of the detector relevant for this analysis have been described in reference [6], as has the trigger for the hadronic events.

Electromagnetic energies are measured by the High density Projection Chamber (HPC) and the Forward Electromagnetic Calorimeter (FEMC). The HPC is a gas sampling calorimeter which measures with high granularity the three-dimensional charge distribution induced by electromagnetic showers, enabling the identification of electrons in a hadronic environment. The HPC covers polar angles, θ, between 40^0 and 140^0. The FEMC is made of lead glass counters covering polar angles 10^0 to 36^0 and 144^0 to 170^0.

Hadron shower energies are measured by the Hadron Calorimeter (HCAL): the instrumented iron return yoke for the magnet, covering polar angles 42.6^0 to 137.4^0 (barrel) and extending for the endcaps from 11.2^0 to 46.5^0 and from to 131.5^0 to 168.8^0.

The muon identification relies mainly on the Muon Chambers, covering polar angles between 53° and 127° in the barrel and between 9° and 43° (137° and 171°) in the forward regions. These consist of layers of drift chambers placed both inside and beyond the iron of the magnet return yoke.

Tracks are measured in a 1.2 Tesla magnetic field by a set of four cylindrical tracking detectors: the Inner Detector (inner radius 12 cm, outer radius 28 cm, covering polar angles between 23^0 and 157^0), the Time Projection Chamber (TPC) (inner radius 30 cm, outer radius 122 cm, covering polar angles between 21^0 and 159^0) and the Outer Detector (inner radius 198 cm, outer radius 206 cm, covering polar angles between 42^0 and 138^0). Additional precise $R\phi$ measurements in the plane perpendicular to the magnetic field are provided by the Vertex Detector (VD). The 1991 and 1992 setup for the VD consisted of three layers of silicon strip detectors, 24 cm long, at radii 6.5 cm, 9 cm and 11 cm, with

an angular acceptance of $27^0 - 153^0$, $37^0 - 143^0$ and $42^0 - 138^0$ respectively. The intrinsic point resolution for single tracks in the transverse plane has been measured to be ± 8 μm. With the VD included in the track fit, the momentum resolution is $\Delta p/p \simeq 0.0008\ p$ (p in GeV/c) [7].

Only charged particles fulfilling the following criteria were used:

- impact parameter less than 5 cm from the beam axis in the xy plane and within 10 cm of the crossing point in z (along the beam direction);
- momentum p larger than 0.2 GeV/c;
- relative error on track momentum less than 100%;
- measured track length above 30 cm;
- polar angle satisfying $|\cos\theta| \leq 0.93$.

Hadronic events were selected, with an efficiency of $(96.4 \pm 0.2)\%$, by requiring:

- at least 7 charged particles;
- total energy of charged particles larger than 15% (or total energy of charged plus neutral particles larger than 30%) of the centre of mass energy (assuming all charged particles to be pions).

The resulting data sample has a small contamination from $\tau^+\tau^-$ events (about 0.1%), and negligible contamination from beam-gas scattering and $\gamma\gamma$ interactions. For the 1991 and 1992 running periods totals of 256350 and 720360 events were left after these cuts.

To compute efficiencies and estimate backgrounds simulated events were generated by means of the Parton Shower model from JETSET 7.3 [8] followed by full detector simulation [9]. These events were processed with the same chain of analysis programs as real data. Samples of 472000 (650000) $Z \to q\bar{q}$ and 11000 (25000) $Z \to b\overline{b} \to J/\psi\ X$ simulated events were used for the 1991 (1992) data sample.

3 Lepton identification and J/ψ, ψ' and χ_c reconstruction

3.1 Muon selection

Muon candidates with momentum above 2 GeV/c were selected by extrapolating charged particle tracks through the calorimeters and performing a χ^2 fit to the positions of hits in the muon chambers. Track measurement errors, multiple scattering errors and chamber resolutions were included. This analysis selected on χ^2 so as to optimize the muon detection efficiency. Within the geometrical and kinematic acceptance an identification efficiency of 90% was measured for muons in $Z \to \mu^+\mu^-$ data. A charged hadron had a probability of 1.5% to fake a muon. The simulation gave an efficiency of $(86.0 \pm 1.3)\%$ for identifying muons (above 2 GeV/c) from J/ψ decays, giving both muons within the selection described in section 2.

To recover lost muons, mainly those outside the geometrical acceptance of the Muon Chambers, information from the HCAL was used, requiring a muon-like energy deposition in at least 3 of its 4 layers. These additional muons improve the efficiency to $(93.4 \pm 1.4)\%$ with a slightly increased background.

3.2 Electron selection

Only charged particles with momentum greater than 2 GeV/c were considered as electron candidates.

The HPC is the key device for the electron identification and is described in detail elsewhere [6]. It has a relative energy resolution of $\pm 5.5\%$ and a spatial resolution in the z-direction (beam axis) of ± 2 mm for an electron with 45.6 GeV/c momentum.

For electron identification a fit was made to the longitudinal shower profile measured in the 9 HPC layers. In addition the energy, position and direction measurements of the shower in the HPC, together with the independent parameters from the track fit, were used to determine an overall probability for a shower to originate from an electron.

A second completely independent way to distinguish between electrons and hadrons is to use the dE/dx measurement in the TPC.

Requiring both the HPC and TPC measurements led to typical efficiencies for electron identification of 50% at 2 GeV/c, increasing to 70% for momentum larger than 6 GeV/c, in the barrel region ($|\cos\theta| < 0.72$). The misidentification rate for charged hadrons inside a jet was found to be 0.4% .

However for this analysis the emphasis was put on the maximization of efficiency. Therefore, in order to look for J/ψ candidates, any particle passing the previous selection was combined with a second particle for which only a shower in the HPC or a dE/dx measurement compatible with the electron hypothesis was required.

3.3 J/ψ reconstruction

J/ψ candidates were reconstructed using the $\mu^+\mu^-$ (1991+1992 data) and e^+e^- (1992 data only) decay channels. For each J/ψ candidate a three-dimensional secondary vertex fit was performed and the particle momenta recomputed including the vertex constraint. Each pair was required:

- to have both decay particles in the same hemisphere (defined by the thrust axis);
- to have a minimum total reconstructed momentum ($p_{J/\psi}$) of 5 GeV/c;
- to have a probability for the secondary vertex fit greater than 1% .

In addition, the hemisphere containing the J/ψ candidate was required to include more than 75% of the beam energy - measured by summing the neutral and charged energies (with a resolution of ± 5.6 GeV). This selection suppresses contributions with two cascade semi-leptonic decays $b \to c l \bar{\nu}$, $c \to s \bar{l} \nu$ where the hemisphere containing the cascade has 10 GeV less energy on average. From simulation, the efficiency of this selection for J/ψ from b decays is 93% and it removes 50% of the cascade events which amounted to 40% of the total background before this cut.

The invariant-mass spectrum for muon (electron) candidate pairs is shown in Fig. 1a (1c). To evaluate the number of J/ψ events, the signal shape was modelled with a Gaussian and the background with an exponential plus a constant term (see fitted curves) in a binned fit. The results of the fits on data for the $J/\psi \to \mu^+\mu^-$ and $J/\psi \to e^+e^-$ samples are shown in table 1. The measured masses and widths are in agreement with what is expected from simulation.

For the decay $J/\psi \to e^+e^-$, the dilepton mass spectrum has a significant low mass tail due to final state radiation and bremsstrahlung. From the simulation, it was estimated that the bremsstrahlung energy losses in the detector move 23% of $J/\psi \to e^+e^-$ events to below 2.8 GeV/c^2.

J/ψ decay (data)	Number of J/ψ	Mass σ (GeV/c^2)	Mass (MC) σ (MC) (GeV/c^2)
$J/\psi \to \mu^+\mu^-$ (91+92)	112±12	3.089±0.005 0.042±0.006	3.087 ± 0.001 0.045 ± 0.001
$J/\psi \to e^+e^-$ (1992)	41±12	3.023±0.024 0.089±0.032	3.017 ± 0.009 0.099 ± 0.008

Table 1: J/ψ reconstruction results for the data and simulation (MC). The fitted errors are shown.

For the $J/\psi \to \mu^+\mu^-$ ($J/\psi \to e^+e^-$) samples the detailed composition of the background obtained from the simulation is shown in Fig. 1a (1c). The number of background events and the shape of their mass distribution are in agreement with the predictions. The slope parameter in the exponential term of the background was also checked to be compatible with that for $e^\pm\mu^\mp$ pairs (Fig. 1b). The background level is 19% (57%) for the $J/\psi \to \mu^+\mu^-$ ($J/\psi \to e^+e^-$) sample, in the mass region between 3.02 and 3.16 GeV/c^2 (2.80 and 3.25 GeV/c^2).

The background subtracted normalized momentum ($x_p = p_{J/\psi}/p_{beam}$) distribution for $J/\psi \to \mu^+\mu^-$ candidates in the above mass range is shown in Fig. 2. The background has been subtracted using combined same sign $\mu\mu$ and opposite sign $e\mu$ combinations in the mass range 2.9 to 3.3 GeV/c^2. The prediction for the process $Z \to b\overline{b} \to J/\psi\ X$ from the simulation is shown.

3.4 ψ' reconstruction

The search for ψ' used the channel $\psi' \to J/\psi(\to \mu^+\mu^-)\pi^+\pi^-$ [†]. After selecting J/ψ candidates in the mass range from 3.02 to 3.16 GeV/c^2, the invariant-mass of the lepton pairs was constrained to the Particle Data Group (PDG) value of the J/ψ mass of 3.097 GeV/c^2 [10]. The criteria used to select ψ' candidates were the following:

- the impact parameter of each pion must be compatible with the reconstructed J/ψ secondary vertex at the level of three standard deviations, and the probability $P(\chi^2)$ to form a vertex with four tracks must be larger than 1%;
- the invariant-mass of the two pions must be greater than 0.4 GeV/c^2 (according to the experimental results from [11], theoretically discussed in [12]).

The invariant-mass spectrum of $J/\psi\ \pi^+\pi^-$ combinations is shown in Fig. 3. According to the simulation, 86 % of the signal is expected between 3.678 and 3.694 GeV/c^2, with a width of 4.5 MeV. There are 6 events in this range, whereas only 0.6 background events are expected, interpolating a flat background. Thus there are $5.4 \pm 2.5 \pm 1.0$ ψ' candidates with weighted mean mass 3.685±0.002 GeV/c^2. The systematic error is mainly connected to the choice of the mass window.

3.5 χ_c reconstruction

The search for χ_c mesons used $\chi_c \to J/\psi(\to \mu^+\mu^-)\ \gamma$ decays, with J/ψ candidates in the same mass range as in the ψ' analysis with the invariant-mass of the lepton pair constrained to the J/ψ PDG mass value. $\chi_{c0}(3415)$ has a negligible branching ratio into

[†] ψ' mesons were also searched for in the channel $\psi' \to \mu^+\mu^-$, without finding a signal. This is not surprising given the branching ratio measured in the $J/\psi\pi\pi$ channel (see section 4).

J/ψ. The mass difference between $\chi_{c1}(3510)$ and $\chi_{c2}(3555)$ is less than the expected mass resolution in the simulation, therefore, in the following the notation χ_c means both resonances. The reconstruction of the photons used the HPC. For this analysis, only photons in the same hemisphere as the J/ψ and satisfying the following criteria were used:

- photon energy greater than 1.1 GeV;
- photon pointing to the interaction region ($\Delta\theta \leq 9^0$ and $\Delta\phi \leq 16^0$, where $\Delta\theta$ and $\Delta\phi$ refer to differences between photon direction as measured from HPC alone and the direction constructed from the shower starting point and the J/ψ vertex);
- no combination with any other photon giving an invariant-mass in the range (50-230) MeV/c^2 , to suppress the background from π^0 decays.

The combined effect of these cuts in the simulation (MC) is illustrated in Fig. 4a and 4b. The invariant-mass spectrum for J/ψ γ combinations accepted after cuts, in real data, is shown in Fig. 4c with fit results superimposed. While the signal was fitted with a Gaussian, the shape of the background under the signal was extracted from simulation (Fig. 4b) and fitted to a convolution of an exponential and a Gaussian, leaving as a free parameter the normalization of the background. The number of χ_c candidates is 6.4 ± 2.7, with fitted mass $m_{\chi_c} = 3.511 \pm 0.018$ GeV/c^2 and $\sigma_{\chi_c} = 0.024 \pm 0.012$ GeV/c^2.

The same fit to simulated data gives $m_{\chi_{c1}} = 3.502 \pm 0.010$ GeV/c^2, $\sigma_{\chi_{c1}} = 0.054 \pm 0.009$ GeV/c^2, assuming the measured χ_{c1} production rate (see section 5.3) and $m_{\chi_c} = 3.514 \pm 0.008$ GeV/c^2, $\sigma_{\chi_c} = 0.057 \pm 0.008$ GeV/c^2, assuming an equal production rate for χ_{c1} and χ_{c2}, as in reference [13].

The measured m_{χ_c} value is consistent with the expected one, while the width, σ_{χ_c}, is some 2 standard deviations smaller than expected.

4 Inclusive branching fractions

After fitting, the background subtracted J/ψ signals contain 112.0 ± 12.4 events for the $J/\psi \to \mu^+\mu^-$ sample and 41.1 ± 12.2 events for the $J/\psi \to e^+e^-$ sample. The inclusive J/ψ branching ratio was estimated from the formula:

$$Br(Z \to J/\psi X) = \frac{N_{J/\psi}}{N_{Z_{had}} \times \frac{\Gamma_Z}{\Gamma_{had}}} \times \frac{\epsilon_{had}}{\epsilon_{J/\psi}} \times \frac{1}{Br(J/\psi \to l^+l^-)} \qquad (4)$$

where $N_{J/\psi}$ is the number of J/ψ found in the $N_{Z_{had}}$ hadronic decays of Z, and ϵ_{had} is the hadronic Z tagging efficiency $(96.4 \pm 0.2)\%$, $\epsilon_{J/\psi}$ is the $J/\psi \to \mu^+\mu^-$ reconstruction efficiency evaluated from the $b \to J/\psi$ simulated data $((36.1 \pm 0.5)\%)$ or the $J/\psi \to e^+e^-$ reconstruction efficiency $((13.6 \pm 0.8)\%)$. The e^+e^- efficiency is significantly lower due to the low mass tail of the dilepton spectrum and the reduced efficiency and acceptance of the electron tagging (barrel region only).

For $Br(J/\psi \to \mu^+\mu^-, e^+e^-)$ the MARK III value $(5.91 \pm 0.23)\%$ [11] has been taken, and $\Gamma_Z = 2489 \pm 7$ MeV, $\Gamma_{had} = 1740.3 \pm 5.9$ MeV which are the current LEP averages[14], have been used.

The results are:

$$Br(Z \to J/\psi\ X) = (3.62 \pm 0.40 \pm 0.34 \pm 0.14) \times 10^{-3} \quad (\mu^+\mu^-),$$

$$Br(Z \to J/\psi\ X) = (4.79 \pm 1.42 \pm 0.52 \pm 0.19) \times 10^{-3} \quad (e^+e^-).$$

The first error quoted is statistical only, the second error is the systematic error, which includes two kinds of contributions (see table 2): one due to *selection cuts* (leptons and J/ψ momentum, hemisphere energy and vertex reconstruction), which are common to electrons and muons, and a lepton dependent contribution including the *efficiency* evaluation (lepton identification algorithm, detector status and Monte carlo statistics) and the *fitting procedure* of the mass spectrum (obtained by varying the parametrization of the background). The third error (also shown in table 2) comes from the uncertainty on the branching ratio $Br(J/\psi \to l^+l^-)$.

Source	$\mu^+\mu^-$	e^+e^-
Selection cuts	5.3	5.3
Efficiency + fitting procedure	7.7	9.4
$Br(J/\psi \to l^+l^-)$	3.9	3.9
Total	10.1	11.5

Table 2: Systematic uncertainties (%) in the $Z \to J/\psi(\to \mu^+\mu^-)X$ ($Z \to J/\psi(\to e^+e^-)X$) branching ratio measurement.

Computing a weighted average of these results, taking into account the common and independent parts of the systematic errors, the final number is

$$Br(Z \to J/\psi\ X) = (3.73 \pm 0.39 \pm 0.36) \times 10^{-3}$$

The inclusive ψ' and χ_{c1} branching ratios[‡] were estimated using the following formula:

$$Br(Z \to c\bar{c}\ X) = \frac{N_{(c\bar{c})} \times \epsilon_{J/\psi}}{N_{J/\psi} \times \epsilon_{(c\bar{c})}} \times \frac{Br(Z \to J/\psi X)}{Br((c\bar{c}) \to Y)} \tag{5}$$

where $(c\bar{c})$ indicates the ψ' (χ_{c1}) state and Y is the decay channel $J/\psi\ \pi^+\pi^-$ ($J/\psi\ \gamma$). $\epsilon_{\psi'} = (12.2 \pm 0.7)\%$ ($\epsilon_{\chi_{c1}} = (5.5^{+0.9}_{-1.2})\%$) is the reconstruction efficiency of ψ' (χ_{c1}). The values $Br(\psi' \to J/\psi\ \pi^+\pi^-) = (32.4 \pm 2.6)\%$ and $Br(\chi_{c1} \to J/\psi\ \gamma) = (27.3 \pm 1.6)\%$ have been taken from the PDG [10].

For the $J/\psi \to \mu^+\mu^-$ sample, this gives

$$Br(Z \to \psi'\ X) = (1.60 \pm 0.73 \pm 0.33) \times 10^{-3}$$

$$Br(Z \to \chi_{c1}\ X) = (5.0 \pm 2.1^{+1.5}_{-0.9}) \times 10^{-3}$$

where the first error is statistical and the second is systematic and takes into account contributions from the evaluation of background subtraction (ψ'), fitting procedure (χ_c) and branching ratios.

[‡] We have assumed only χ_{c1} production for efficiency evaluation and branching ratio calculation.

5 $B \to J/\psi$ decays

5.1 Average B lifetime

The negligible lifetime of J/ψ mesons implies that the observed secondary vertex is a good estimate of its parent's decay position.

From the fit of the secondary J/ψ vertex and of the primary vertex, the decay length l_{xy} in the transverse plane was computed for each event. The transverse (xy) position of the vertex formed by the two muons was reconstructed with a most probable precision of ± 125 μm along the direction of the primary to secondary vertex, 80% of the events having a better than ± 300 μm error. The mean transverse position of the beam spot was computed for each fill of LEP and used as a constraint for the primary vertex fit for each event. This vertex fit was done in two iterations. The first iteration included all good quality charged particles. The second iteration allowed removal of tracks having a big contribution to the χ^2, and therefore to remove as many of the tracks coming from secondary vertices as possible. The resulting uncertainty on the position of the primary vertex is typically ten times smaller than that on the secondary vertex.

The direction of the jet containing the J/ψ was taken as the direction of the parent b-hadron. In the simulation, the polar angle θ_{jet} coincides with the true polar angle of the parent b-hadron with a mean error of ± 20 mrad.

The three dimensional decay length l was then determined as $l = l_{xy}/\sin\theta_{jet}$. The proper time of each event is defined as $t = l/(\beta\gamma c) = (m_B/p_B) \times l$.

The B boost was estimated as follows. A first estimation of the B momentum (p_B) was obtained by a polynomial parametrization $f(p_{J/\psi})$ as a function of the J/ψ momentum in the simulation. It was then used as a starting point for the B jet reconstruction. The clustering algorithm used the parameter y, defined as

$$y_{ik} = \left(y_0 - (\frac{M}{P})_{i+k}\right)^2 \qquad \text{where} \qquad y_0 = \frac{< m_B >}{f(p_{J/\psi})}$$

where M and P are the mass and momentum of the cluster $(i + k)$ and $< m_B >= 5.3$ GeV/c^2 is the expected mean mass of b-hadrons. The procedure was initialized by adding to the J/ψ (cluster i) the particle k with momentum greater than 0.5 GeV/c that minimized y_{ik}. The invariant-mass of the cluster $(i + k)$ was calculated considering all charged particles as pions and all neutrals as photons. Other particles were added iteratively as long as $M \leq 5.6$ GeV/c^2.

The resulting mean value of $\frac{M}{P}$ reproduced the true value with a systematic bias of less than 1.5%. The dispersion $\sigma(\frac{M}{P})$ was parameterized using a polynomial function; its mean value was 11%. The proper time was estimated as $t = (\frac{M}{P}) \times l$ of the b-hadron, and the error on the proper time for each event σ_t was taken as the sum in quadrature of the errors from l_{xy}, $(\frac{M}{P})$ and θ_{jet}.

The Figure 5 shows the proper time distribution of the $J/\psi \to \mu^+\mu^-$ candidates in the signal region $3.03 \leq m_{\mu\mu} \leq 3.15$ GeV/c^2 after applying an additional selection consisting of keeping J/ψ candidates with at least two VD hits per muon, to improve the quality of the track extrapolation. This left a total of 80 events, with a background level of (16.5 ± 2.2)%.

In the maximum likelihood fit of the proper time distribution, two terms were used for the signal: a convolution of an exponential decay function and a Gaussian resolution

function given by the estimated errors on the time, σ_t, for the J/ψ coming from B, and a Gaussian distribution only for any possible prompt J/ψ candidates.

Two background components were taken into account: one "flying" background that was included in the fitting function with a term similar to the $B \to J/\psi$ signal but with a different lifetime, and one "non-flying" background which had only a Gaussian form.

The number of free parameters was therefore four: the mean B lifetime, τ_B, the fraction of prompt J/ψ, $f^{pr}_{J/\psi}$, the fraction of background that does not fly, f^{nf}_{bkg}, and the lifetime of the flying background τ_{bkg}. The fraction of background was fixed to 16.5%. The fit was performed simultaneously on the 80 signal region candidates and on 85 events from the side-bands (mass ranges from 2.5 to 2.9 and from 3.3 to 3.5 GeV/c^2). In the fit, τ_{bkg} and f^{nf}_{bkg} were constrained mainly by the side-band data. Also, because of small individual errors on proper times, the correlation between τ_B and $f^{pr}_{J/\psi}$ was found to be low (0.18).

The result was [§]:

$$\tau_B = 1.50^{+0.24}_{-0.22} \text{ ps}$$
$$f^{pr}_{J/\psi} = (7.7^{+6.3}_{-5.4}) \ \%$$
$$\tau_{bkg} = 1.72 \pm 0.23 \text{ ps}$$
$$f^{nf}_{bkg} = (28.5 \pm 5.9)\%$$

The simulation showed the same proportion of "non-flying" background: (27.3±6.6)%. The value of τ_{bkg} was tested to be compatible with the one obtained using $e\mu$ opposite sign combinations in the signal mass region. However, these events were not actually used in the background lifetime fit because of the different quality of reconstruction of electrons and muons. The fitted prompt J/ψ fraction $f^{pr}_{J/\psi}$, at the present level of statistics, is not incompatible with the theoretical predictions of the order of 1%.

The contributions to the systematic error are shown in table 3.

Source	Uncertainty (ps)
Fake J/ψ background	±0.01
B momentum evaluation	±0.02
Decay length resolution	±0.015
Check of the method on MC	±0.015
Total	±0.03

Table 3: Systematic uncertainties in the lifetime determination.

The first component was obtained by varying the level of background within its statistical error; the second one was derived from the Monte Carlo study of the reconstruction of the $\frac{M}{P}$ of the B hadron. The component coming from the decay length resolution resulted from varying the individual errors on the transverse decay length by ±20%. The component "check of the method on Monte Carlo" comes from a test of the complete analysis of the lifetime on two simulated samples generated with two different lifetimes

[§] If the prompt J/ψ contribution, theoretically expected to be small, is forced to zero, the mean B lifetime given by the fit is instead $1.43^{+0.22}_{-0.19}$ ps. On the other hand, fixing the mean B lifetime to $1.582 \pm 0.012 \pm 0.032$ ps as measured by DELPHI [15], one obtains a prompt J/ψ fraction of $(8.1^{+6.3}_{-5.4})$ %.

(1.2 and 1.6 ps). In both cases, the lifetime measured in the simulation agrees with the generated lifetime within statistics; the statistical error on this check is taken as a systematical uncertainty on the measurement in the data. The total systematic error on the evaluation of τ_B was ± 0.03 ps.

Interpreting the prompt J/ψ component as produced by mechanisms (2) or (3), its mean fraction (7.7%) would correspond to a branching ratio $Br(Z \to \text{direct } J/\psi) = 3.8 \times 10^{-4}$ (3.1×10^{-4}) for process (2) (process (3)) .

5.2 Average B lifetime from exclusively reconstructed states

In the J/ψ $(\psi') \to \mu^+\mu^-$ channel, exclusive B candidates were reconstructed using a mass constrained fit on the two leptons from J/ψ. For the charged tracks, associated to the secondary vertex, a probability $P(\chi^2)$ bigger than 1% to form a vertex was required and a minimum momentum between 2 and 5 GeV/c, depending on the chosen channel. Kaons were identified by mean ionization in the TPC and by the barrel RICH detector. Twenty exclusive B meson decay candidates, namely five $B^\pm \to J/\psi K^\pm$, four $B^0 \to J/\psi K^0$, three $B^0 \to J/\psi K^{*0}(K\pi)$, two $B^\pm \to J/\psi K^{*\pm}(K^0_S\pi)$, three $B^\pm \to J/\psi K^{*0}\pi$, one $B^\pm \to J/\psi K^\pm\pi^+\pi^-$, one $B^0 \to \psi'(\to \mu^+\mu^-)K^{*0}$ and one $B_s \to J/\psi\phi$ candidate were reconstructed.

The invariant-mass spectrum observed for all the searched channels is shown in Fig. 6 both for simulation and data. The background is modelled from the inclusive $b \to J/\psi\, X$ simulation using two components with different shapes: one is from B mesons where at least one particle is lost, and the other from genuine J/ψ from B meson decays where one or more charged particle from hadronization is included in the reconstruction. The background from fake J/ψ events is negligible, being at low apparent B mass.

In the mass interval from 5.18 to 5.40 GeV/c^2, there are 15.2 ± 4.5 signal events, with a mean mass in agreement with the nominal B meson mass and 4.8 ± 0.6 background events, which represents (24 ± 3)% of the sample.

The average lifetime of B mesons is estimated by a maximum likelihood fit, with an individual likelihood density given by an exponential convoluted with a Gaussian. The mean resolution on individual times of flight is 0.07 ± 0.01 ps. As in the inclusive lifetime fit, the background lifetime is simultaneously fitted with a similar individual likelihood function using events with invariant-mass between 5.40 and 6 GeV/c^2 and events with wrong charge combination for kaon and pions. The result is:

$$\tau_B = 1.7\,^{+0.6}_{-0.4}\ \pm 0.1 \text{ ps}.$$

The systematic error comes from the exclusive channel composition of the background (0.11 ps), the parametrization of the background lifetime distribution (0.07 ps) and the error on the fraction of background (0.03 ps).

5.3 $b \to (c\bar{c})$ branching ratios

From the value of $\Gamma_{b\bar{b}}/\Gamma_{had} = 0.2200 \pm 0.0027$ (current LEP average [14]), subtracting the $(7.7^{+6.3}_{-5.4})$% prompt component in the J/ψ sample, the branching ratios $Br(b \to (c\bar{c})X)$ are ¶

$$Br(b \to J/\psi\ X) = (1.12 \pm 0.12 \pm 0.10)\%$$

¶ Assuming a null contribution from prompt J/ψ, the branching ratios are instead $Br(b \to J/\psi\, X) = (1.21 \pm 0.13 \pm 0.12)$%, $Br(b \to \psi'\ X) = (0.52 \pm 0.24 \pm 0.11)$% and $Br(b \to \chi_{c1}\ X) = (1.6 \pm 0.7^{+0.5}_{-0.3})$%.

$$Br(b \to \psi' \; X) = (0.48 \pm 0.22 \pm 0.10)\%$$
$$Br(b \to \chi_{c1} \; X) = (1.4 \pm 0.6^{+0.4}_{-0.2})\%.$$

The first two values are consistent with the PDG values of $(1.12 \pm 0.16)\%$ and $(0.46 \pm 0.20)\%$ respectively, despite the fact that the B species content differs between Z and $\Upsilon(4S)$ decays. The third measurement is compatible with ARGUS [16] ($(1.05 \pm 0.35 \pm 0.25)\%$) and L3 [17] ($(2.4 \pm 0.9 \pm 0.2)\%$) measurements.

6 Conclusions

Inclusive J/ψ production from hadronic Z decays has been studied. An analysis of the apparent lifetimes shows a $(7.7^{+6.3}_{-5.4})$ % fraction of prompt J/ψ mesons. Subtracting this prompt J/ψ component, three inclusive branching ratios of $B \to (c\bar{c})$ have been measured with the DELPHI detector:

$$Br(b \to J/\psi \; X) = (1.12 \pm 0.12 \pm 0.10)\%$$
$$Br(b \to \psi' \; X) = (0.48 \pm 0.22 \pm 0.10)\%$$
$$Br(b \to \chi_{c1} \; X) = (1.4 \pm 0.6^{+0.4}_{-0.2})\%.$$

The average b-hadron lifetime was determined as:

$$\tau_B = 1.50^{+0.24}_{-0.21} \pm 0.03 \text{ ps},$$

in good agreement with other LEP results, obtained with the J/ψ tag [3]-[5].

A set of 15 ± 5 B mesons were fully reconstructed. From these events we estimated an average lifetime of B mesons :

$$\tau_B = 1.7^{+0.6}_{-0.4} \pm 0.1 \text{ ps}$$

in agreement with the previous determination.

Acknowledgements

We are greatly indebted to our technical collaborators and to the funding agencies for their support in building and operating the DELPHI detector, and to the members of the CERN-SL Division for the excellent performance of the LEP collider.

References

[1] K. Hagiwara, A. Martin and W. Stirling, Phys. Lett. **B267** (1991) 527 and erratum, Phys. Lett. **B316** (1993) 631;
E. Braaten and T.C. Yuan, Phys. Rev. Lett. **71** (1993) 1673;
E. Braaten and T.C. Yuan, Fermilab-PUB-94/040-T.

[2] V. Barger, K. Cheung and W.Y. Keung, Phys. Rev. **D41** (1990) 1541;
E. Braaten, K. Cheung and T.C. Yuan, Phys. Rev. **D48** (1993) 4230.

[3] D. Buskulic et al. (ALEPH Collaboration), Phys. Lett. **B295** (1992) 396.

[4] G. Alexander et al. (OPAL Collaboration), Phys. Lett. **B266** (1991) 485.

[5] O. Adriani et al. (L3 Collaboration), Phys. Lett. **B288** (1992) 412.

[6] P. Aarnio et al. (DELPHI Collaboration), Phys. Lett. **B240** (1990) 271;
P. Aarnio et al. (DELPHI Collaboration), Nucl. Instr. and Meth. **A303** (1991) 233.

[7] N. Bingefors et al., Nucl. Instr. and Meth. **A328** (1993) 447.

[8] T. Sjöstrand, Comp. Phys. Comm. **27** (1982) 243, ibid. **28** (1983) 229;
T. Sjöstrand and M. Bengtsson, Comp. Phys. Comm. **43** (1987) 367.

[9] 'DELSIM Reference Manual', DELPHI Note 89-68, Sept. 1989.

[10] Particle Data Group, K. Hikasa et al., Phys. Rev. **D45** (1992).

[11] D. Coffman et al. (MARKIII Collaboration), Phys. Rev. Lett. **68** (1992) 282.

[12] L.S. Brown and R.N. Cahn, Phys. Rev. Lett. **35** (1975) 1;
M. Chemtob and H. Navelet, Phys. Rev. **D 41** (1990) 2187;
H-Y. Zhou and Y-P. Kuang, Phys. Rev. **D 44** (1991) 756.

[13] G.T. Bodwin, E. Braaten, T.C. Yuan and G.P. Lepage, Phys. Rev. **D46** (1992) 3703.

[14] The LEP collaborations and the LEP Electroweak Working Group, CERN-PPE/93-157 (Aug. 1993).

[15] P. Abreu et al. (DELPHI Collaboration), CERN PPE 94-24, submitted to Zeit. Phys. C.

[16] H. Albrecht et al. (ARGUS Collaboration), Phys. Lett. **B277** (1992) 209.

[17] O. Adriani et al. (L3 Collaboration), Phys. Lett. **B317** (1993) 467.

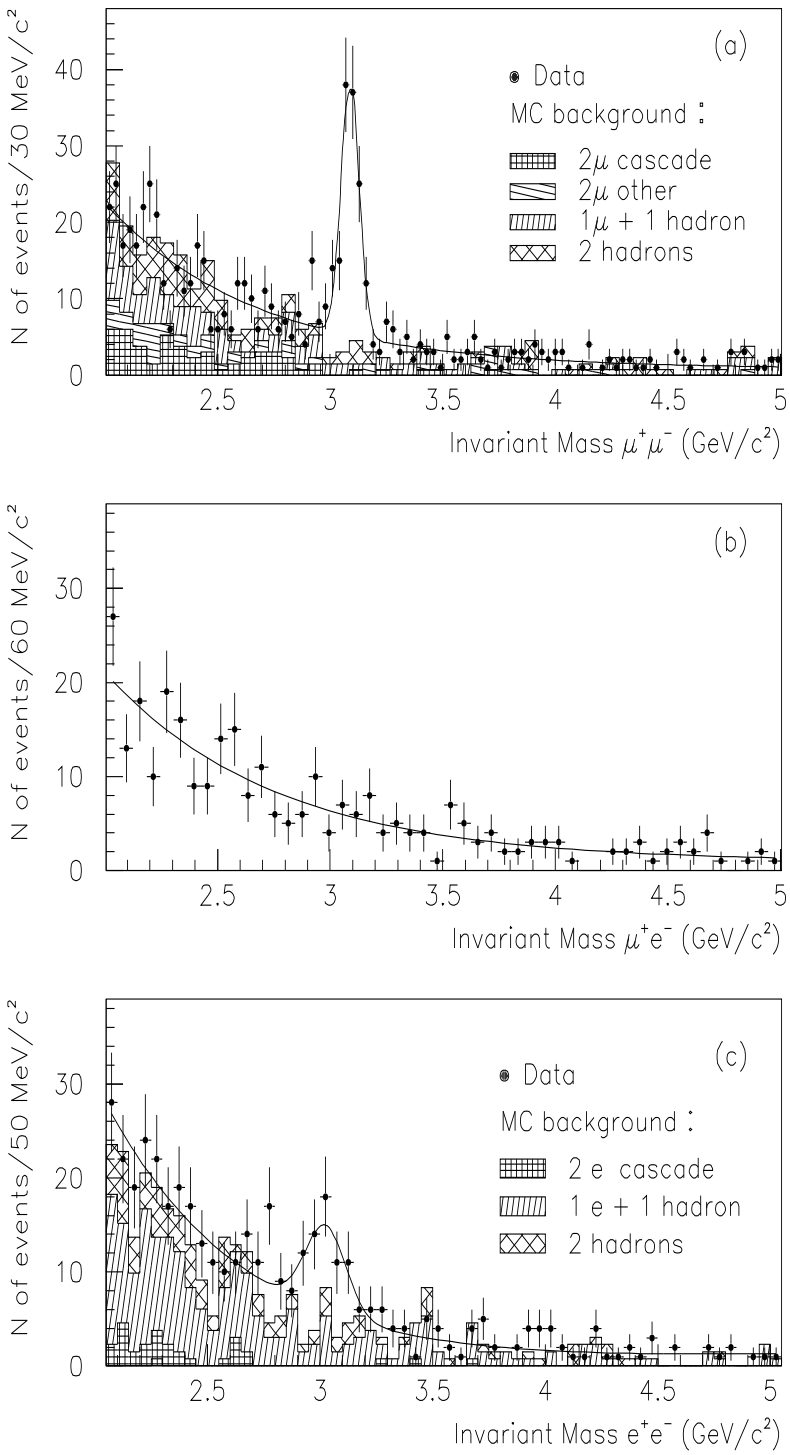

Figure 1: (a) $\mu^+\mu^-$, (b) $e^\pm\mu^\mp$ and (c) e^+e^- invariant-mass distributions (same sign $\mu\mu$ and ee distributions are similar to the $e^\pm\mu^\mp$ one). The background estimates, from an inclusive $Z \to q\bar{q}$ simulation, are shown as hatched histograms. The curves show the fits to the data, as explained in the text.

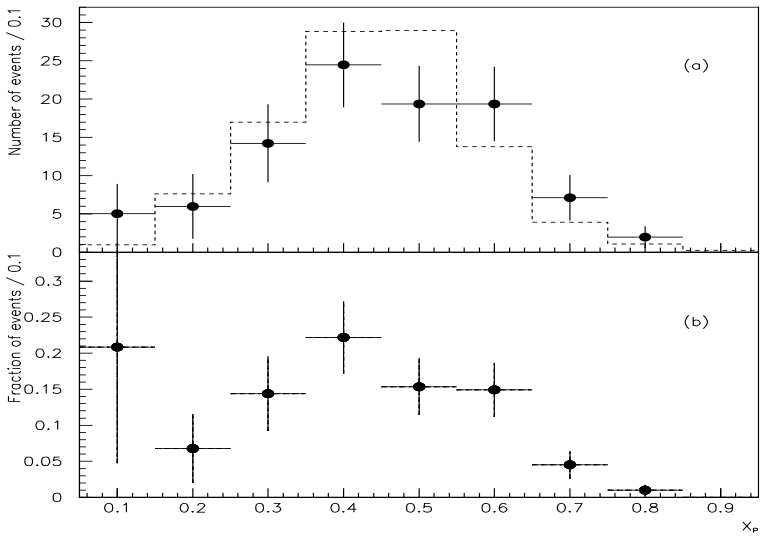

Figure 2: (a) the background subtracted x_p distribution for the $J/\psi \to \mu^+\mu^-$ sample. The errors are statistical only. The histogram shows the simulation for the process $Z \to b\bar{b} \to J/\psi X$. (b) the same plot, corrected for the experiment acceptance.

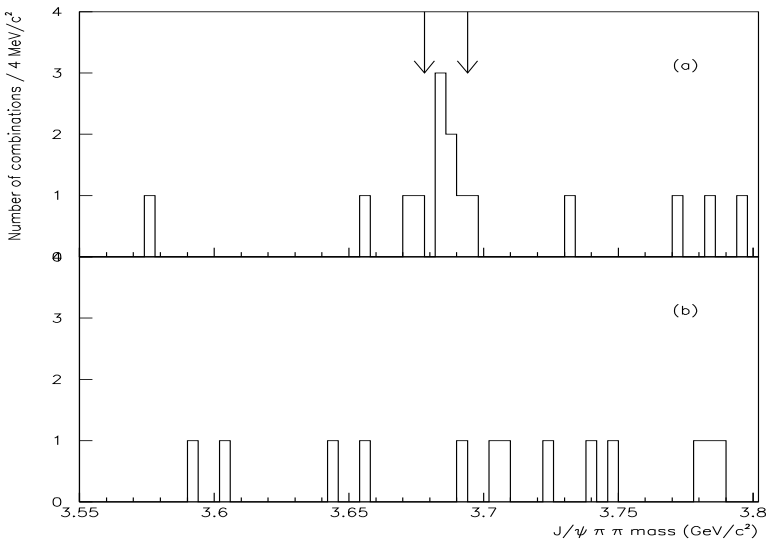

Figure 3: $J/\psi\pi\pi$ invariant-mass combinations for (a) opposite sign pions (arrows show the signal mass interval considered, defined by simulation); (b) same sign pions.

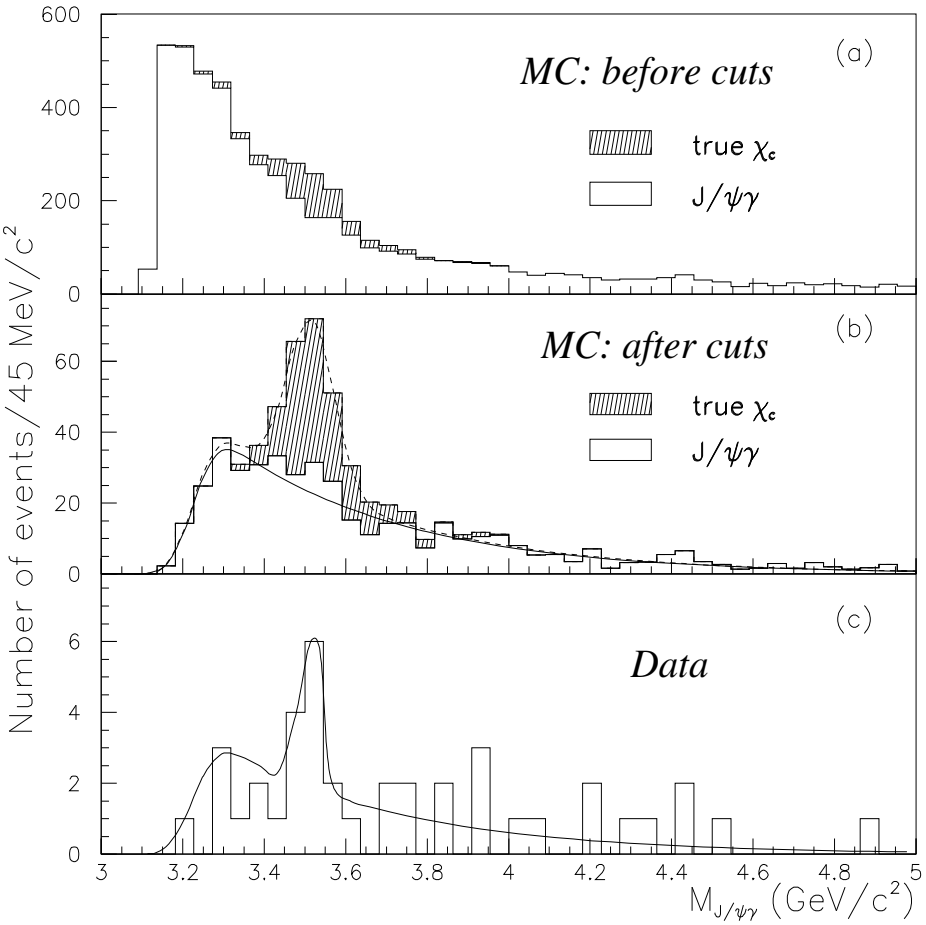

Figure 4: (a) Simulated J/ψ γ invariant-mass distribution, before imposing cuts on photons. J/ψ selection is already done, including the choice of the mass interval. (b) same as above after applying the cuts. The full curve shows a fit of the background and the dotted curve is the fit including a Gaussian distribution for the signal. The background was estimated using a combination of true J/ψ and random γ's. (c) For real data: the corresponding plot to (b), where the full curve shows the fit of signal plus background.

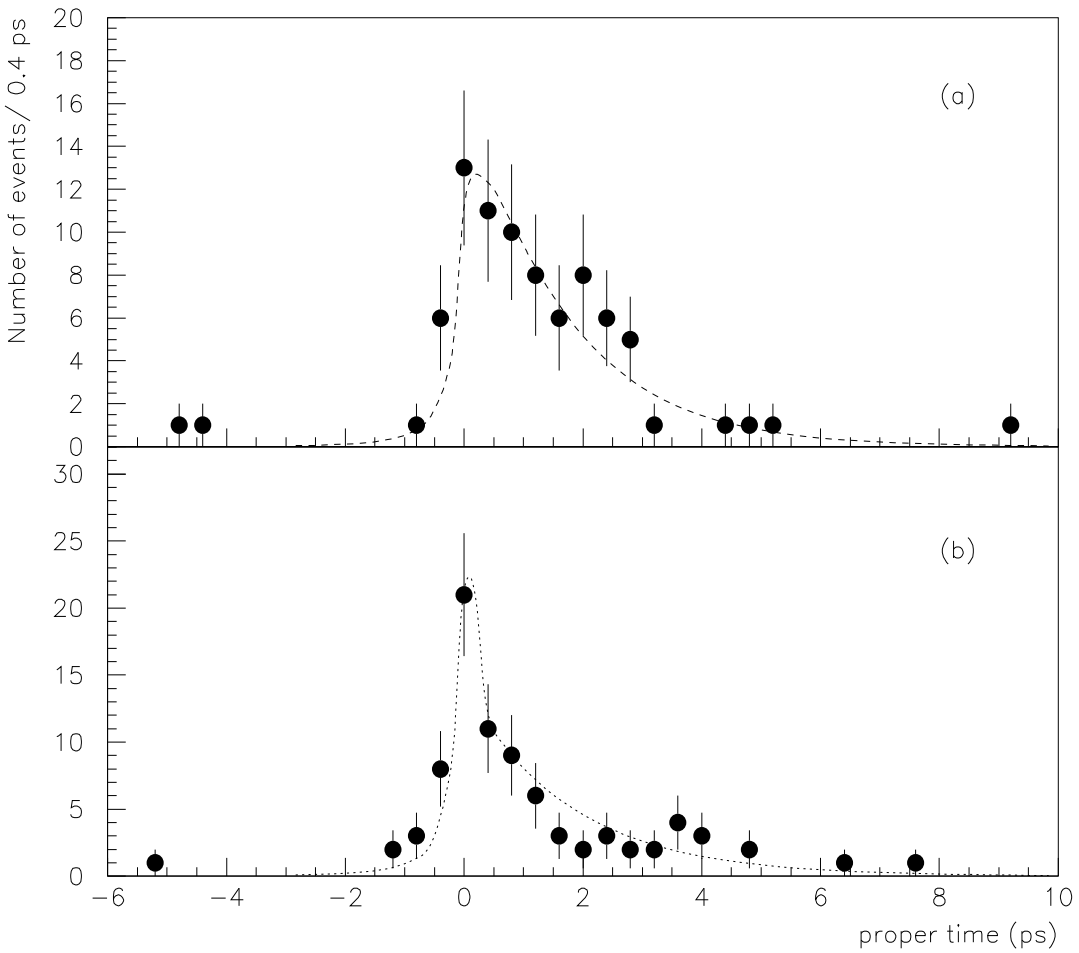

Figure 5: Proper time distribution for the J/ψ candidates (muon data only). The curve shows the result of the unbinned maximum likelihood fit to determine the lifetime: a) signal events; b) sideband events. The "lifetime" of the background is due to semileptonic decays of heavy flavours.

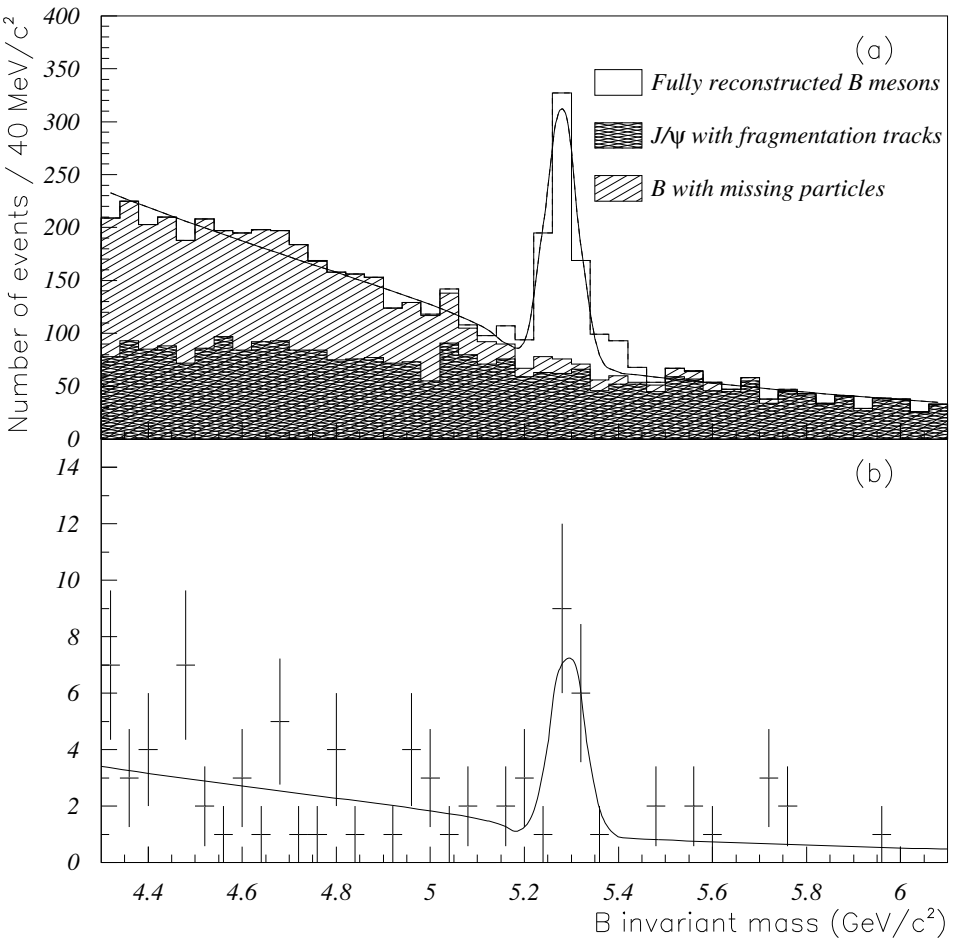

Figure 6: (a) simulation of $Z \to J/\psi(\psi')X$: sum of B invariant-mass distribution for all selected exclusive decay channels with the two relevant components of the background. The curve shows a fit with a Gaussian for the B decays plus background. (b) Same distribution for 1991 and 1992 real data. The curve shows the fit to the data with the slopes of the backgrounds and the width of the signal fixed to the simulated data above.